METHODS AND APPLICATIONS OF ANALYSIS.
Vol. 15, No. 4, pp. 539–556, December 2008

008

SHAPE ANALYSIS BY CONFORMAL MODULES*

WEI ZENG†, LOK MING LUI‡, XIANFENG GU§, AND SHING-TUNG YAU¶

Abstract. All the surfaces in real life are Riemann surfaces, therefore with conformal structures. Two surfaces share the same conformal structure, if there exists a conformal (angle-preserving) mapping between them. Conformal modules are the complete invariants of conformal structures, which can be treated as shape descriptors for shape analysis applications.

This work focuses on the computational methods of conformal modules for genus zero surfaces with boundaries, including topological quadrilaterals, annuli, multiply connected annuli. The algorithms are based on both holomorphic 1-forms and discrete curvature flows, which are rigorous and practical. The conformal module shape descriptors are applied for shape classification and comparison. Experiments on surfaces acquired from real world demonstrate the efficiency and efficacy of the conformal module method.

Key words. Conformal module, holomorphic 1-form, curvature flow, shape classification, shape analysis.

AMS subject classifications. 30F20, 68R99

1. Introduction.

Recently, the $3D$ geometric acquisition technology has been becoming much mature. The demands for geometric surfaces classification and indexing have been increased greatly. It is urgent to develop automatic, rigorous and efficient algorithms to compute geometric invariants of general shapes for classification and analysis purposes. In recent decades, there has been a lot of research into shape invariants [1, 2, 3, 4, 5].

According to Klein's Erlange program, different geometries study the invariants under different transformation groups. Shapes can be classified by different geometric invariants. For the purpose of shape classification, the topological invariants are too coarse, which are not discriminative; Riemannian geometric invariants are too refined, it is difficult to compare directly. Conformal geometry is more rigid than topology and more flexible than Riemannian geometry. Conformal geometry offers a promising methodology for shape classification and indexing. Recently, conformal geometry has been successfully applied for surface matching and registration [6, 7, 8, 9, 10, 11].

A conformal mapping between two surfaces preserves angles. Two surfaces are conformally equivalent, if there exists a conformal mapping between them. Therefore, all surfaces in real life can be classified by conformal equivalence relation. If two surfaces are conformally equivalent, then the area distortion (conformal factor) can be used to further differentiate them, which determines the Riemannian metric. In theory, two conformally equivalent surfaces, with the same conformal factor and mean curvature at the corresponding points, differ solely by a rigid motion.

In the current work, we focus on computing the conformal invariants, the so called conformal module, for genus zero surfaces with all kinds of topologies. The

*Received April 16, 2009; accepted for publication September 8, 2009.

†Department of Computer Science, State University of New York at Stony Brook, Stony Brook, NY 11794-4400, USA (zengwei@cs.sunysb.edu).

‡Department of Mathematics, Harvard University, Cambridge, MA 02138, USA (malmlui@math.harvard.edu); and Department of Mathematics, University of California, Los Angeles, CA 90095-1555, USA (malmlui@math.ucla.edu).

§Department of Computer Science, State University of New York at Stony Brook, Stony Brook, NY 11794-4400, USA (gu@cs.sunysb.edu).

¶Department of Mathematics, Harvard University, Cambridge, MA 02138, USA (yau@math.harvard.edu).

major theoretic results postulate the following facts:

1. All genus zero closed surfaces are conformally equivalent. The conformal factor and mean curvature determine the surface uniquely up to a rigid motion, which has been used as the shape descriptors in [9].
2. All genus zero surfaces with a single boundary are conformally equivalent, all of them can be conformally mapped to the unit disk by a Riemann mapping.
3. All genus zero surfaces with a single boundary and four marked points on the boundary, *topological quadrilaterals*, are conformally equivalent to rectangles, with different height-width ratios. The ratio is called the *conformal module*, which uniquely determines the conformal structure of the surface. Figures 1 and 2 illustrate the concept.
4. All genus zero surfaces with two boundaries, *topological annuli*, are conformally equivalent to canonical planar annuli bounded by two concentric circles with different ratios between the inner and outer radii. The ratio is called the *conformal module*, which solely determines the conformal structure of the surface. Figure 3 demonstrates the conformal module for topological annuli.
5. All genus zero surfaces with multiple boundaries, *topological multiply connected annuli*, are conformally equivalent to the unit disk with circular holes. The conformal mapping is unique up to a Möbius transformation. The centers and radii of the circular holes are the conformal invariants. Figure 4 shows the conformal invariants of multiply connected annuli.

For high genus surfaces, the computation of conformal invariants requires sophisticated techniques from Teichmüller theory and hyperbolic geometry. Especially, discrete hyperbolic surface Ricci flow is essential. We refer readers to [12] for more details.

The major contributions of the current work are the following general framework and novel algorithms:

1. A framework to use conformal invariants as the shape descriptors for classification and analysis.
2. An algorithm for computing conformal modules for topological quadrilaterals based on exact harmonic 1-forms.
3. An algorithm for computing conformal modules for topological annuli based on holomorphic 1-forms.
4. An algorithm for computing conformal invariants for multiply connected annuli based on discrete surface curvature flow.

The paper is organized in the following way: Section 2 will briefly introduce the most related works in the literature; Section 3 will introduce the major theoretic concepts from differential geometry, Riemann surface theory; details of algorithms are explained in Section 4; experimental results are reported in Section 5; the conclusion and future direction are discussed in Section 6.

2. Related work. Our work proposes to compute the conformal modules as shape descriptors for genus zero surfaces with boundaries, for shape classification purposes. The research literature on shape descriptors is vast. Here, we will focus only on the recent shape descriptors which are most relevant to our work using conformal geometry, and methods for computing conformal maps.

2.1. Conformal geometry related shape descriptors. shape descriptors are to extract meaningful and simplified representations from the 3D model based on the geometric and topological characteristics of the object, for the application of 3D shape

classification and matching. Comprehensive surveys of different shape descriptors and evaluations of their performance are given by [13], [14], [15] and [16].

Shape descriptors based on conformal geometry for classification is proposed in [17], where the conformal invariants are represented as the period matrices. Geodesic spectrum of surfaces under their uniformization metrics is applied as the shape descriptors in [18]. 3D surface matching based on conformal mapping is proposed in [19, 20].

Laplace-Beltrami operator related descriptors are presented in [21] and [22], which are invariant to isometric deformations and tolerant to quasi-isometric deformations. Pose-invariant shape descriptors based on conformal geometry are introduced in [23], where the histogram of the conformal factor computed from surface uniformization metric is applied as shape descriptor. Recently, Jin et.al [12] applied Teichmüller space coordinates as shape descriptors for high genus surfaces using hyperbolic metric, which are succinct, discriminating and intrinsic, invariant under the rigid motions and scalings.

2.2. Conformal mapping methods. There are many algorithms for conformal surface parameterization in the literature. Comprehensive reviews can be found in [24] and [25]. Here we focus on the approaches to computing holomorphic differential 1-forms and discrete curvature flow.

Holomorphic 1-form. Global method without segmentation is proposed by Gu et al. [26]. They used holomorphic one-forms as the underlying tool, which is general for surfaces with arbitrary topologies. One-form has also been used for vector fields decomposition and smoothing [27]. Discrete one-forms on meshes were studied in [28]. Tong et al. [29] used harmonic one-forms for surface parameterization. They enlarged the space of harmonic one-forms by allowing additional singular points on the surface. Kalberer et al. applied one-forms for surface parameterization combining with branch covering in [30], where the parameter lines are governed by a given frame field. In [31] Fisher et al. used one-forms for designing tangent vector fields on surfaces with complicated topologies.

Curvature flow. The theoretic foundations of discrete surface curvature flow have been introduced in [32, 33, 34, 35]. The engineering applications have been introduced in [36, 37, 38, 39, 40]. As a powerful tool for shape analysis, Ricci curvature flow [36, 37] has been successfully used for the applications in computer graphics and vision, such as surface matching and registration [20, 41], classification and indexing [12].

3. Theoretic background. This section briefly introduces the background knowledge in conformal geometry, necessary for the discussion in the work. For more details, we refer readers to [42] for Riemann surface theory, [43] for Teichmüller theory and [44] for differential geometry.

3.1. Conformal structure. Suppose S is a topological surface. U_α is an open set on S, $\phi_\alpha : U_\alpha \to \mathbb{C}$ maps each point in U_α to its *local coordinates* on the complex plane. (U_α, ϕ_α) is a *local coordinates chart*. An *atlas* $\mathfrak{A} = \{(U_\alpha, \phi_\alpha)\}$ is a collection of local coordinate charts, which cover the whole surface.

Suppose S is embedded in $\mathbb{R}^3$, therefore it has the induced Euclidean metric $\mathbf{g}$. Suppose on a local chart (U_α, ϕ_α) with local coordinates z_α,

$$\mathbf{g} = e^{2\lambda} dz_\alpha d\bar{z}_\alpha,$$

then z_α is an *isothermal coordinates*. If all the local coordinates in $\mathfrak{A}$ are isothermal, then the atlas is called a *conformal structure*.

Let (U_α, ϕ_α) and (U_β, ϕ_β) be two local charts in a conformal atlas, with local coordinates z_α, z_β respectively, then the *coordinates transition function* $\phi_{\alpha\beta} = \phi_\beta \circ \phi_\alpha^{-1} : z_\alpha \to z_\beta$ is *holomorphic*, meaning $\frac{\partial \phi_{\alpha\beta}}{\partial \bar{z}_\alpha} = 0$.

Another interpretation of conformal structure is more useful for understanding the curvature flow method. Let S be a topological surface, we consider all the possible Riemannian metrics on S, $G = \{\mathbf{g}\}$. Two metrics $\mathbf{g}_1, \mathbf{g}_2$ are *conformally equivalent*, $\mathbf{g}_1 \sim \mathbf{g}_2$, if there exists a function $\lambda : S \to \mathbb{R}$, such that $\mathbf{g_1} = e^{2\lambda}\mathbf{g}_2$. Intuitively, the angle values measured by $\mathbf{g}_1$ equals to that by $\mathbf{g}_2$. Then each conformal equivalence class of the Riemannian metrics in $G/\sim$ is a conformal structure.

3.2. Conformal mapping. A mapping between two Riemann surfaces $f : S_1 \to S_2$ is *conformal*, if it satisfies the following condition. Arbitrarily choosing a local isothermal coordinates of S_1, (U_α, ϕ_α), a local isothermal coordinates of S_2, (V_β, ϕ_β), then the local presentation of f is $\phi_\beta \circ f \circ \phi_\alpha^{-1}$ is holomorphic.

Conformal mappings preserve angles. Namely, if there exists a conformal mapping between S_1 and S_2, then S_1 and S_2 have the same conformal structure.

3.3. Conformal invariants. In order to verify whether two Riemann surfaces are conformally equivalent or not, it is unnecessary to really find the conformal mapping between them, which is still a widely open problem for general surfaces. Instead, one can compute some geometric quantities determined by the conformal structure of the surface, which are called the *conformal invariants*. By comparing the conformal invariants, it is easy to verify whether two Riemann surfaces are conformally equivalent or not.

All genus zero closed surfaces are conformally equivalent to the unit sphere, therefore, all of them are conformally equivalent. All genus zero surface with a single boundary can be conformally mapped to the unit disk by a Riemann mapping, therefore, all topological disks are conformally equivalent. A topological triangle is a topological disk with three marked boundary points $T(p_1, p_2, p_3)$. Then we can find a unique Riemann mapping $\phi : T(p_1, p_2, p_3) \to \mathbb{D}$, such that ϕ maps p_1, p_2, p_3 to $1, i, -1$. Therefore, all topological triangles are conformally equivalent.

DEFINITION 3.1 (Topological Quadrilateral). *Suppose S is a surface of genus zero with a single boundary, and four marked boundary points p_1, p_2, p_3, p_4 sorted counter-clock-wisely. Then S is called a topological quadrilateral, and denoted as $Q(p_1, p_2, p_3, p_4)$.*

The following theorem states the complete conformal invariants of a topological quadrilateral.

THEOREM 3.2 (Conformal Module). *Suppose $Q(p_1, p_2, p_3, p_4)$ is a topological quadrilateral with a Riemannian metric, then there exists a unique conformal map $\phi : S \to \mathbb{C}$, such that ϕ maps Q to a rectangle, $\phi(p_1) = 0$, $\phi(p_2) = 1$. The height of the image rectangle is called the conformal module of $Q(p_1, p_2, p_3, p_4)$.*

Similarly, conformal module can be defined for topological annuli.

DEFINITION 3.3 (Topological Annulus). *Suppose S is a surface of genus zero with two boundaries, then S is called a topological annulus.*

The complete conformal invariant for a topological annulus is postulated by the following theorem.

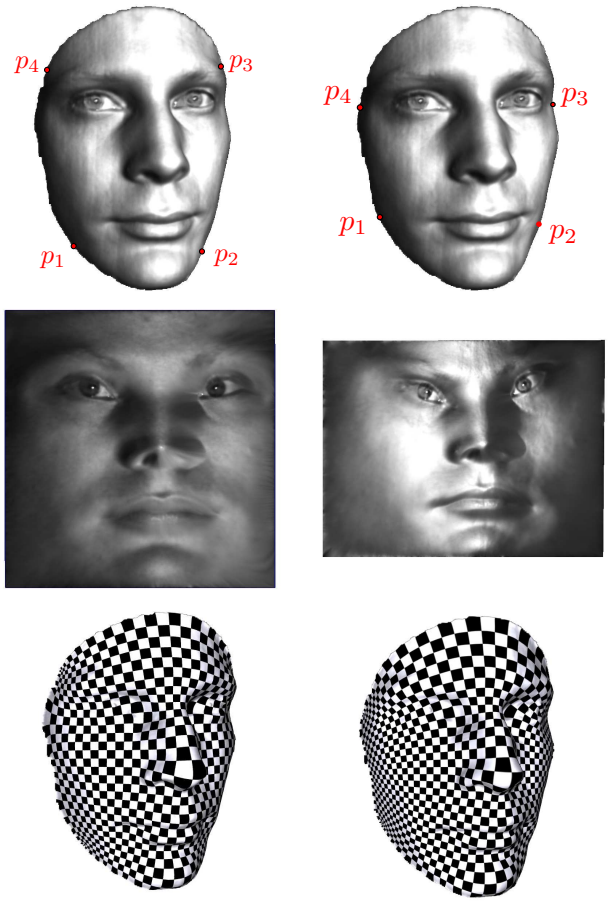

FIG. 1. *Conformal modules for topological quadrilaterals. Same surface with different marked points have different conformal modules, 1.02866 for (a) and 0.770193 for (b).*

THEOREM 3.4 (Conformal Module). *Suppose S is a topological annulus with a Riemannian metric, the boundary of S are two loops $\partial S = \gamma_1 - \gamma_2$. Then there exists a conformal map $\phi : S \to \mathbb{C}$, which maps S to the canonical annulus, $\phi(\gamma_1)$ is the unit circle, $\phi(\gamma_2)$ is another concentric circle with radius r. Then r is the conformal module of S. The mapping ϕ is unique up to a rotation.*

For a multiply connected annulus, the conformal module is more complicated. All the conformal mappings from a unit disk to itself are *Möbius transformations*, and can be represented as

$$z \to e^{i\theta} \frac{z - z_0}{1 - \bar{z}_0 z},$$

where z_0 is an interior point in the unit disk.

DEFINITION 3.5 (Multiply Connected Annulus). *Suppose S is a surface of genus zero with multiple boundaries, then S is called a multiply connected annulus.*

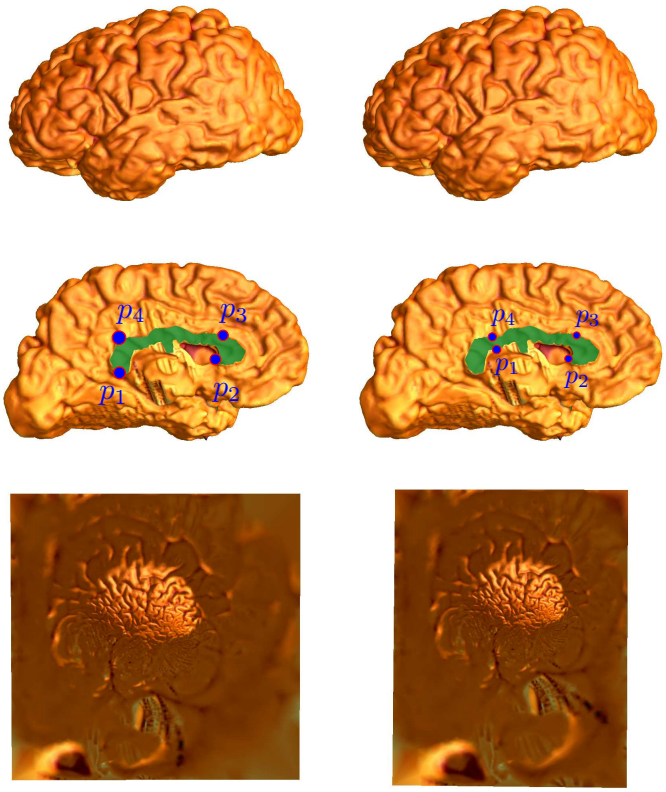

(a) (b)

FIG. 2. *Conformal modules for brain cortex surfaces, which are topological quadrilaterals. Same surface with different marked points have different conformal modules, 1.00898 for (a) and 1.27361 for (b).*

THEOREM 3.6. *Suppose S is a multiply connected annulus with a Riemannian metric, then there exists a conformal map $\phi : S \to \mathbb{C}$, which maps S to the unit disk with circular holes. The radii and centers of the inner circles are conformal invariants of S. Such kind of conformal mappings are unique up to Möbius transformations.*

3.4. Holomorphic 1-forms.

Harmonic functions. Let $f : S \to \mathbb{R}$ be a function defined on the surface, then the *harmonic energy* of f is defined as

$$E(f) = \int_S |\nabla f|^2 dA,$$

where ∇f is the gradient of f, dA is the area element on S. The *harmonic function* is the critical point of the harmonic energy, and satisfies the Laplace equation $\Delta f = 0$, where Δ is the Laplace-Beltrami operator on S.

Harmonic 1-form. Suppose S is a Riemann surface with an conformal atlas. Let (U_α, ϕ_α) be a local coordinate chart, the local coordinates are $x_\alpha + iy_\alpha$. A *differential*

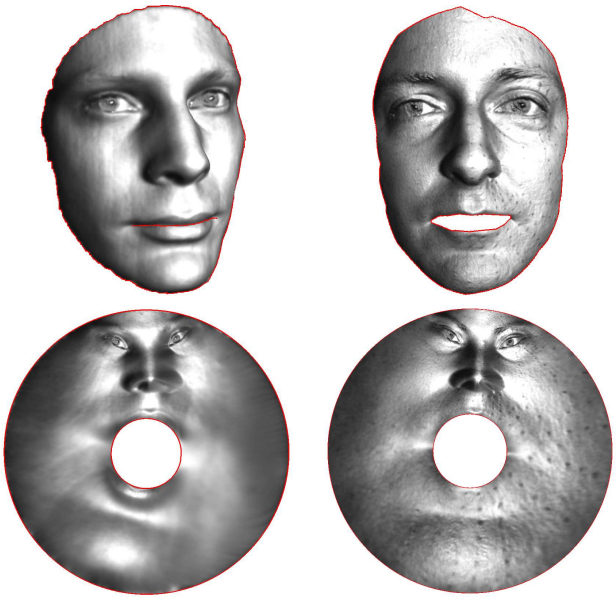

(a) (b)

FIG. 3. *Conformal modules for topological annulus, 0.246647 for (a) and 0.262499 for (b).*

1-form has the local representation $\tau = f_\alpha dx_\alpha + g_\alpha dy_\alpha$. On another chart (U_β, ϕ_β) with local coordinates $x_\beta + iy_\beta$, $\tau = f_\beta dx_\beta + g_\beta dy_\beta$. such that

$$\begin{pmatrix} f_\beta \\ g_\beta \end{pmatrix} = \begin{pmatrix} \frac{\partial x_\alpha}{\partial x_\beta} & \frac{\partial y_\alpha}{\partial x_\beta} \\ \frac{\partial x_\alpha}{\partial y_\beta} & \frac{\partial y_\alpha}{\partial y_\beta} \end{pmatrix} \begin{pmatrix} f_\alpha \\ g_\alpha \end{pmatrix}.$$

A differential 1-form is a *harmonic 1-form*, if locally, it is the gradient of a harmonic function.

Intuitively, the *Hodge star* rotates a differential 1-form τ by a right angle, on each local chart, it is defined ${}^*\tau = -g_\alpha dx_\alpha + f_\alpha dy_\alpha$. We also say $*\tau$ is *conjugate* to τ.

Holomorphic 1-form. Let ω be a complex-valued differential form on the Riemann surface S, such that on each local chart (U_α, ϕ_α) with isothermal coordinates z_α, ω has local representation $\omega = g_\alpha(z_\alpha)dz_\alpha$, where g_α is holomorhpic, then ω is called a *holomorphic 1-form*. A holomorphic 1-form can be decomposed to two harmonic 1-forms, conjugate to each other, namely $\omega = \tau + i^*\tau$,

All the holomorphic 1-forms form a group, which is isomorphic to the first cohomology group of the Riemann surface.

3.5. Surface Ricci curvature flow. Let S be a surface embedded in $\mathbb{R}^3$. S has a Riemannian metric induced from the Euclidean metric of $\mathbb{R}^3$, denoted by $\mathbf{g}$. Suppose $u : S \to \mathbb{R}$ is a scalar function defined on S, then $\bar{\mathbf{g}} = e^{2u}\mathbf{g}$ is a conformal metric on S.

The Gaussian curvatures will also be changed accordingly. The Gaussian curvature will become

$$\bar{K} = e^{-2u}(-\Delta_{\mathbf{g}} u + K),$$

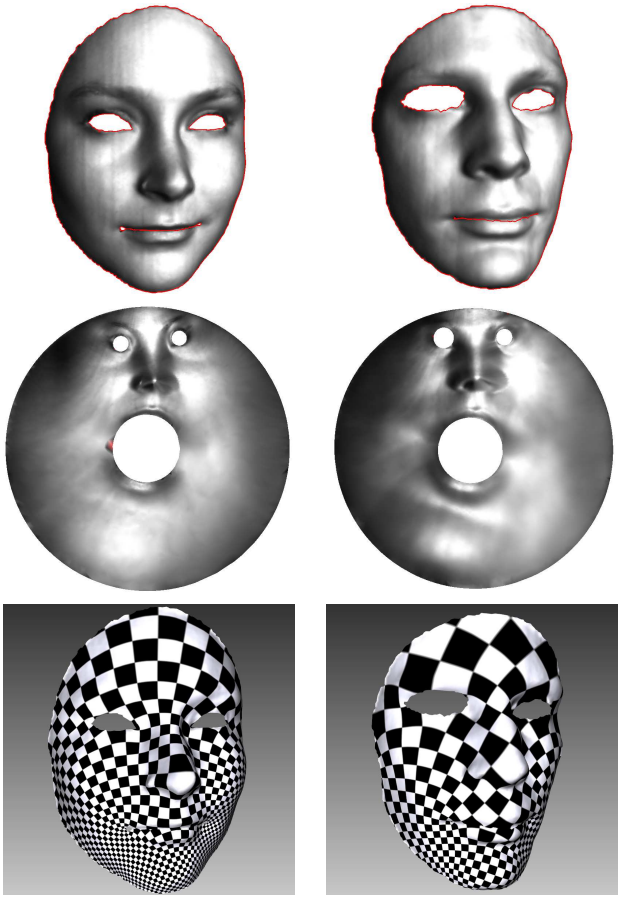

(a) (b)

FIG. 4. *Conformal modules for multiply connected annuli (see Table 2 for experimental results).*

where $\Delta_{\mathbf{g}}$ is the Laplacian-Beltrami operator induced by the original metric $\mathbf{g}$. The above equation is called the *Yamabe equation*. Yamabe equation can be solved using *Ricci flow* method. The Ricci flow deforms the metric $\mathbf{g}(t)$ according to the Gaussian curvature $K(t)$ (induced by $\mathbf{g}(t)$), where t is the time parameter

$$\frac{dg_{ij}(t)}{dt} = 2(\bar{K} - K(t))g_{ij}(t).$$

Ricci flow method can be applied to design Riemannian metrics with prescribed Gaussian curvatures. For example, if the target curvature $\bar{K}$ is zero on every interior point, then the surface can be flattened onto a planar domain with the resulting metric $e^{2u}\mathbf{g}$.

4. Algorithms. This section introduces the algorithms for computing conformal invariants for genus zero surfaces with various topologies.

All surfaces are represented as triangular meshes, piecewise linearly embedded in $\mathbb{R}^3$. We use V, E, F to represent the vertex, edge and face sets. We use v_i to denote

the vertex, $[v_i, v_j]$ for an oriented edge from v_i to v_j, and $[v_i, v_j, v_k]$ for a face with vertices v_i, v_j, v_k, sorted counter-clock-wisely.

4.1. Topological quadrilateral. Given a triangular mesh Q of genus zero, with a single boundary. Four boundary vertices p_1, p_2, p_3, p_4 are chosen as the marked points. We want to find a conformal mapping $\phi : Q \to \mathbb{C}$, which maps Q to a planar rectangle. Assume the boundary of Q consists of four segments $\partial Q = \gamma_1 + \gamma_2 + \gamma_3 + \gamma_4$, such that

$$\partial\gamma_1 = p_2 - p_1, \partial\gamma_2 = p_3 - p_2,$$
$$\partial\gamma_3 = p_4 - p_3, \partial\gamma_4 = p_1 - p_4.$$

Then we compute two harmonic functions $f_1, f_2 : Q \to \mathbb{R}$, such that

$$\left\{\begin{array}{lcl} \Delta f_1 & = & 0 \\ f_1|_{\gamma_1} & = & 0 \\ f_1|_{\gamma_3} & = & 1 \end{array}\right. \quad \left\{\begin{array}{lcl} \Delta f_2 & = & 0 \\ f_2|_{\gamma_2} & = & 0 \\ f_2|_{\gamma_4} & = & 1 \end{array}\right. .$$

We use the cotan formula [45] to approximate the Laplace-Beltrami operator. Ba-

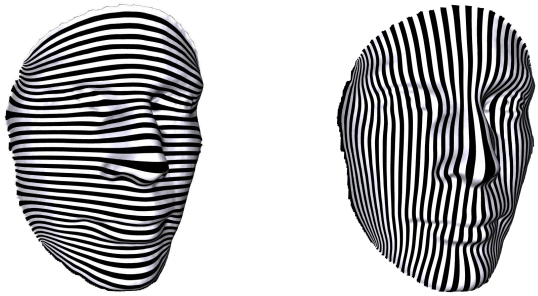

FIG. 5. *Level sets of harmonic functions f_1 and f_2.*

sically, for each edge $[v_i, v_j]$, the two adjacent triangles are $[v_i, v_j, v_k]$ and $[v_j, v_i, v_l]$, the angles against the edge are θ_{ij}^k and θ_{ji}^l in each triangle respectively, then

$$w_{ij} = \cot\theta_{ij}^k + \cot\theta_{ji}^l. \tag{1}$$

Then the Laplacian of a function $f : V \to \mathbb{R}$ is defined as

$$\Delta f(v_i) = \sum_{[v_i,v_j]\in E} w_{ij}(f(v_i) - f(v_j)).$$

Then ∇f_1 and ∇f_2 are two exact harmonic 1-forms. We need to find a scalar λ, such that ${}^*\nabla f_1 = \lambda\nabla f_2$. This can be achieved by minimizing the following energy

$$E(\lambda) = \sum_{[v_i,v_j,v_k]\in F} |\nabla f_1 - \lambda\mathbf{n} \times \nabla f_2|^2 A_{ijk},$$

where ∇f_1 and ∇f_2 are the constant gradient vector of f_1 and f_2 on the face $[v_i, v_j, v_k]$; $\mathbf{n}$ is the normal vector to the face, A_{ijk} is the area of the face. By solving a linear equation, λ can be obtained.

The the desired holomorphic 1-form $\omega = \nabla f_1 + i\lambda\nabla f_2$. Then the conformal mapping $\phi : Q \to \mathbb{C}$ is given by $\phi(p) = \int_q^p \omega$, where q is the base point, the path from q to p is arbitrarily chosen.

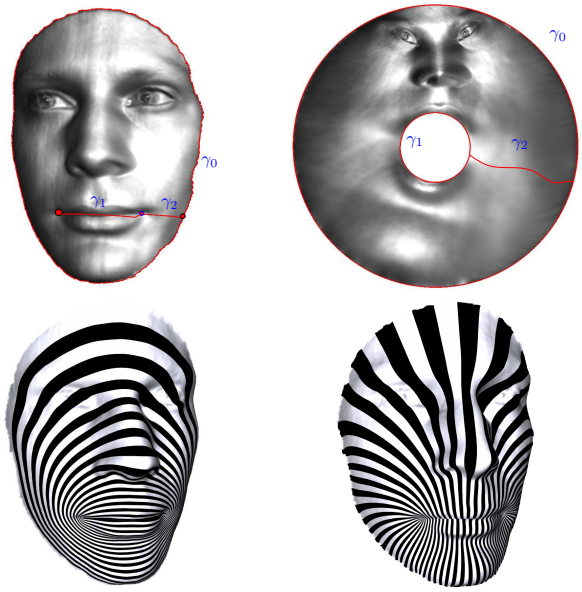

FIG. 6. *Harmonic 1-forms. Top row, the cut on the surface. Bottom row, the level sets of the harmonic 1-form* ∇f *and its conjugate harmonic 1-form* $\lambda(\nabla g_0 + \nabla g_1)$.

4.2. Topological annulus. Suppose S is a topological annulus, with boundaries $\partial S = \gamma_0 - \gamma_1$ as shown in figure 6. First, we compute a path γ_2 connecting γ_0 and γ_1. Then we compute a harmonic function $f : S \to \mathbb{R}$, such that

$$\begin{cases} f_{\gamma_0} &= 0 \\ f_{\gamma_1} &= 1 \\ \Delta f &= 0 \end{cases}.$$

The level set of f is shown in Figure 6. Then ∇f is a harmonic 1-form.

We slice the surface along γ_2 to get a new surface $\tilde{S}$ with a single boundary. γ_2 becomes two boundary segments γ_2^+ and γ_2^- on $\tilde{S}$. Then we compute a function $g_0 : \tilde{S} \to \mathbb{R}$, such that

$$\begin{cases} g_0|_{\gamma_2^+} &= 1 \\ g_0|_{\gamma_2^-} &= 0 \end{cases}$$

g_0 takes arbitrary value on other vertices. Therefore ∇g_0 is a closed 1-form defined on S. Then we find another function $g_1 : S \to \mathbb{R}$, such that $\nabla g_0 + \nabla g_1$ is a harmonic 1-form $\nabla \cdot (\nabla g_0 + \nabla g_1) = 0$.

Then we need to find a scalar λ , such that ${}^*\nabla f = \lambda(\nabla g_0 + \nabla g_1)$ using the similar method as for topological quadrilaterals. The holomorphic 1-form is given by

$$\omega = \nabla f + i\lambda(\nabla g_0 + \nabla g_1).$$

Let $Img(\int_{\gamma_0} \omega) = k$, the conformal mapping from S to a canonical annulus is given by

$$\phi(p) = \exp^{\frac{2\pi}{k} \int_q^p \omega},$$

where q is the base point, the path from q to p is arbitrarily chosen.

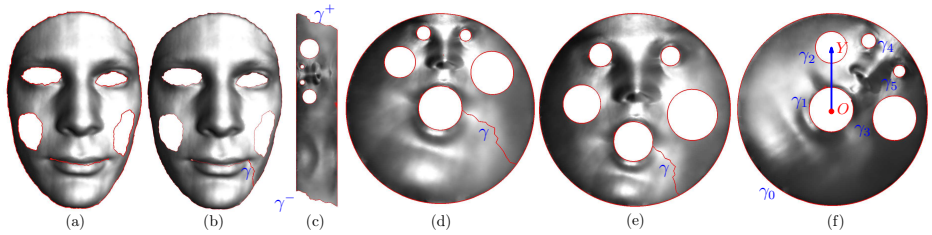

FIG. 7. *Computing process for the conformal invariants of a multiply connected annulus. (a) the input surface with* 6 *boundaries. (b) a cut path* γ *connecting the outer boundary and the longest inner boundary. (c) the flat metric, obtained by curvature flow, which flattens the surface to a parallelogram on the plane. (d) the complex exponential map that maps (c) to an annulus. (e) the result after a Möbius transformation. (f) the canonical map for computing conformal modules using a Möbius transformation.*

4.3. Multiply connected annulus. Discrete curvature flow method is applied for computing the conformal invariants of the multiply connected annuli. On a triangle mesh, the *discrete metric* is the edge length function $\ell : E \to \mathbb{R}^+$ satisfying triangle inequality. The *vertex discrete curvature* is defined as angle deficiency,

$$K_i = \begin{cases} 2\pi - \sum_{[v_i,v_j,v_k]\in F} \theta_i^{jk} & v_i \notin \partial M \\ \pi - \sum_{[v_i,v_j,v_k]\in F} \theta_i^{jk} & v_i \in \partial M \end{cases}$$

where θ_i^{jk} is the corner angle at v_i in the face $[v_i, v_j, v_k]$, ∂M is the boundary of M. Let $\mathbf{u} : V \to \mathbb{R}$ be the discrete conformal factor. The edge length of $[v_i, v_j]$ is defined

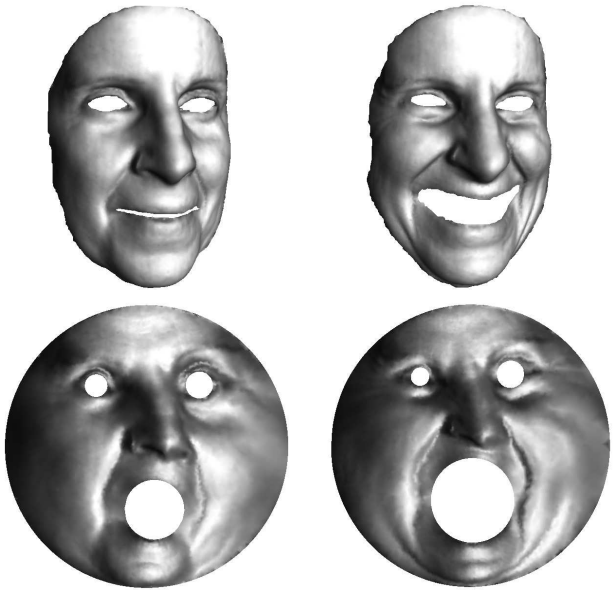

FIG. 8. *Conformal modules for multiply connected annuli (see Table 2 for experimental results). It is obvious that, the human face surfaces with different expressions are not conformally equivalent. Therefore, expression change is not a conformal transformation.*

as

$$\ell_{ij} := \exp(u_i)\exp(u_j)\ell^0_{ij},$$

where ℓ^0_{ij} is the original edge length in $\mathbb{R}^3$. The discrete Yamabe flow is defined as

$$\frac{du_i}{dt} = \bar{K}_i - K_i,$$

with the constraint $\sum_i u_i = 0$. The discrete Yamabe flow converges, and the final discrete metric induces the prescribed curvature. The detailed proof can be found in [34].

The curvature flow is the gradient flow of the following convex energy,

$$E(\mathbf{u}) = \int_{\mathbf{u}_0}^{\mathbf{u}} \sum_{v_i \in V} (\bar{K}_i - K_i) du_i,$$

where $\mathbf{u}_0 = (0, 0, \cdots, 0)$, as described in [36], [34] and [38]. The energy can be minimized using Newton's method directly, where the Hessian matrix is exactly the discrete Laplace-Beltrami operator in Eqn. 1.

Figure 7 illustrates the processing pipeline. Let S be a multiply connected annulus, its boundary consists of n loops, $\partial S = \gamma_0 - \gamma_1 - \gamma_2 \cdots - \gamma_n$. where γ_k's are sorted by their total lengths.

The target curvature is set in the following way:

1. For all interior vertices $v_i \notin \partial S$, $\bar{K}(v_i)$ is zero.
2. For all vertices on γ_0 or γ_1, $\bar{K}(v_i)$ is zero.
3. Let $v_i \in \gamma_k, k \neq 0, 1$, suppose the total length of γ_k under the current metric is $|\gamma_k|$, the two boundary edges attaching to v_i on γ_k are l_i and l_{i+1}, then set

$$\bar{K}(v_i) = -\pi \frac{|l_i| + |l_{i+1}|}{|\gamma_k|}.$$

Note that in the curvature flow, the edge lengths are changing, therefore $\bar{K}(v_i)$ are also time variant.

By running discrete curvature flow with time variant target curvature, the procedure will converge, and a unique flat metric will be obtained. Then we find a shortest path γ_2 connecting γ_0 and γ_1, slice S along γ_2 to get a surface $\tilde{S}$. The flat metric will flatten $\tilde{S}$ onto a planar parallelogram with circular holes. Then we use an exponential map to map the parallelogram to an annulus with circular holes. Finally, we use Yamabe flow to adjust the metric, to make each boundary to be a circle. Figure 8 shows the conformal mapping between multiply connected annuli, which are human faces with different expressions with eyes and mouth removed. They are mapped to the planar unit disk with circular holes. The different radii of the mouth circle indicate the fact that the expression change is not conformal.

5. Experimental results. All the algorithms are implemented using generic C++ on Windows XP platform. The linear systems are solved using Matlab C++ library. All the experiments are conducted on a PC with $3.60GHz$ dual CPUs and 3.00 GB memory.

The surface data are captured by structured light 3D scanner [46], which is capable of capturing high resolution with high speed. The medical imaging data, such as brain

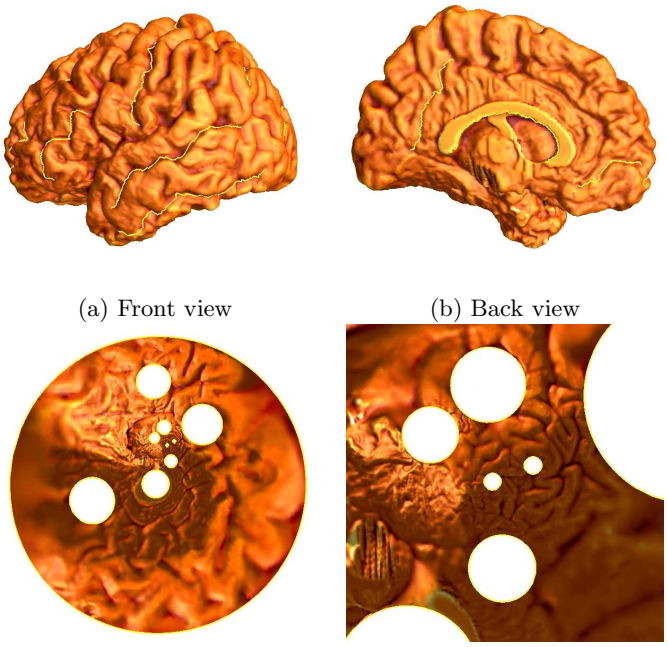

(a) Front view (b) Back view

(c) Planar Image (d) Zoomed in

FIG. 9. *A brain cortex surface is sliced open along* 9 *sulci landmarks in (a) and 1 base boundary in (b). The conformal module is computed using curvature flow method. The planar image and its zoomed-in are shown in (c) and (d).*

cortex surfaces, are reconstructed from MRI images. Table 1 shows the running time for conformal modules of different geometric data using different algorithms.

Experimental results on conformal modules for topological quadrilaterals are reported in Figures 1 and 2. The four corner points along the boundaries are marked in the figures. It is clear that the same geometric surface with different markers have different conformal modules. Furthermore, as shown in Figure 1, if the original surface is symmetric, and the markers are symmetric, then the conformal mapping preserves symmetry.

The conformal modules for topological annuli are shown in Figures 3 and 6. The human face surfaces with mouth cuts are topological annuli, and are conformally mapped to planar annuli. The outer radii equal to one, the inner radii indicate the conformal invariants.

Experimental results on multiply connected annuli are reported in Figures 4, 7, 8 and 9. Each surface is conformally mapped to the unit disk with circular holes inside. The mapping is not unique, different mappings differ by a Möbius transformation. We use the following procedure to remove the Möbius ambiguity. Suppose $\partial M = \gamma_0 - \gamma_1 - \cdots - \gamma_n$, where γ_0 is the outer boundary, γ_k's are sorted in the descending order of their hyperbolic lengths.

We map the outer boundary γ_0 to the unit circle, and use Möbius transformation to move the center of γ_1 to the origin, the center of γ_2 to the imaginary axis. The conformal invariants are defined on this canonical setting. Suppose each boundary γ_k is mapped to a circle $(\mathbf{c}_k, r_k)$, where $\mathbf{c}_k$ is the center, r_k is the radius, then the

conformal invariants are represented as

$$\{r_1, (y_2, r_2), (\mathbf{c}_3, r_3), \cdots, (\mathbf{c}_n, r_n)\}. \tag{2}$$

The processing pipeline is illustrated in Figure 7, where the conformal modules are computed on the canonical map shown in (f). Table 2 lists conformal invariants for each surface.

In Figure 8, we can obviously see that the human face surfaces with different expressions are not conformally equivalent. The L^2 distance between the conformal invariants is 0.069546.

TABLE 1
Running Time for Computing Conformal Modules

Mesh	Figure	Faces	Verts	Bnds	Topology	Time(s)
Alex1	Fig.1a	160058	80598	1	quadrilateral	82
Alex2	Fig.1b	160058	80598	1	quadrilateral	88
Brain1	Fig.2a	58558	29393	1	quadrilateral	28
Brain2	Fig.2b	58558	29393	1	quadrilateral	27
Alex3	Fig.3a, 6	160056	80598	2	annulus	107
Luke	Fig.3b	265478	133759	2	annulus	136
Sophie	Fig.4a	19960	10204	4	multi-connect	52
Alex	Fig.4b	24096	12321	4	multi-connect	48
Alex4	Fig.7	22455	11555	6	multi-connect	40
Anna1	Fig.8a	19984	10212	4	multi-connect	42
Anna2	Fig.8b	19992	10227	4	multi-connect	43
Brain	Fig.9	13168	66549	10	multi-connect	204

The experiments are performed on a dual Xeon(TM) CPU 3.60 GHz, 3.00 GB memory PC.

6. Conclusion. This paper introduces the computational algorithms for a novel shape descriptor, conformal modules for topological quadrilaterals, annuli and multiply connected annuli. The computational algorithms are based on discrete holomorphic 1-forms and discrete curvature flow methods. The computational algorithms are automatic, rigorous and efficient. The conformal invariants can be treated as the fingerprints of the shapes, and applied for shape classification and geometric database indexing.

The algorithms for computing the conformal modules for quadrilaterals and annuli are linear, which are efficient and robust. The requirement to the triangulation quality is low. In contrast, the curvature flow method for multiply connected annuli is highly non-linear, which is as robust as the linear method. The requirements for the triangulations heavily depend on the target curvature. It will be an important direction to establish the theoretic analysis and develop practical algorithm to automatically improve the tessellation quality for curvature flow method.

The relation between the linear method and non-linear method will be another direction for further exploration. For topological annuli, both methods give equivalent results. Curvature flow method is flexible for arbitrary topologies,and holomorphic forms are efficient. It is highly desirable to combine them together.

In the future, we plan to use our conformal module algorithm for large scale geometric database indexing and many other real applications in engineering fields.

TABLE 2
Conformal Modules for Genus Zero Surfaces with Boundaries

Bnd	Sophie Fig.4a	Alex Fig.4b
γ_1	0.237656	0.233511
γ_2	(0.809342) 0.052511	(0.818536) 0.072878
γ_3	(0.656531 -0.384748) 0.055294	(0.720324 0.418042) 0.056624
Bnd	Anna1 Fig.8a	Anna2 Fig.8b
γ_1	0.266628	0.360004
γ_2	(0.798269) 0.051485	(0.798602) 0.053412
γ_3	(0.714065 -0.372099) 0.041063	(0.735581 -0.344529) 0.035383
Bnd	Alex4d Fig.7d	Alex4e Fig.7e
γ_1	0.232286	0.232227
γ_2	(0.647122) 0.166061	(0.646042) 0.166510
γ_3	(-0.085231 0.662051) 0.226530	(-0.108128 0.654063) 0.229110
γ_4	(0.711377 0.393154) 0.074814	(0.703591 0.402676) 0.075556
γ_5	(0.396639 0.711987) 0.061296	(0.378273 0.718480) 0.062258

Bnd	Brain Fig.9
γ_1	0.227251
γ_2	(0.810980) 0.064359
γ_3	(0.408802 -0.390732) 0.122533
γ_4	(0.675160 -0.154978) 0.047408
γ_5	(0.405547 -0.153151) 0.045023
γ_6	(0.582150 -0.202912) 0.027341
γ_7	(0.479104 -0.106130) 0.029712
γ_8	(0.486479 -0.216819) 0.008887
γ_9	(0.508601 -0.179890) 0.008237

$\{\gamma_i\}$ boundaries sorted by hyperbolic length.
γ_1: $[r_1]$, γ_2: $[(v_2)\ r_2]$, γ_i: $[(u_i\ v_i)\ r_i]$.

Acknowledgement. We warmly thank Prof. Paul M. Thompson for his valuable advice and friendly help. The brain data used in this work were provided by Center for Computational Biology (CCB), Laboratory of Neuroimaging, UCLA.

REFERENCES

[1] R. CAMPBELL AND P. FLYNN, *A survey of free-form object representation and recognition techniques,* CVIU, 81 (2001), pp. 166–210.
[2] J. WYNGAERD, L. GOOL, R. KOCH, AND M. PROESMANS, *Invariant-based registration of surface patches,* ICCV99, vol. I, pp. 301–306.
[3] S. RUIZ-CORREA, L. SHAPIRO, AND M. MEILA, *A new paradigm for recognizing 3d object shapes from range data,* ICCV03, vol. II, pp. 1126–1133.
[4] D. HUBER, A. KAPURIA, R. DONAMUKKALA, AND M. HEBERT, *Parts-based 3d object classification,* CVPR04, vol. II, pp. 82–89.
[5] S. BIASOTTI, D. GIORGI, M. SPAGNUOLO, AND B. FALCIDIENO, *Reeb graphs for shape analysis and applications,* Theoretical Computer Science, 392 (2008), pp. 1–3.
[6] B. LEVY, S. PETITJEAN, N. RAY, AND J. MAILLOT, *Least squares conformal maps for automatic texture atlas generation,* SIGGRAPH02, pp. 362–371.
[7] D. ZHANG AND M. HEBERT, *Harmonic maps and their applications in surface matching,*

CVPR99, vol. II, pp. 524–530.
[8] E. Sharon and D. Mumford, *2d-shape analysis using conformal mapping,* CVPR04, vol. II, pp. 350–357.
[9] X. Gu and B. C. Vemuri, *Matching 3d shapes using 2d conformal representations,* MICCAI, Lectures Notes in Computer Science, 3216 (2004), pp. 771–780.
[10] S. Wang, Y. Wang, M. Jin, X. D. Gu, and D. Samaras, *Conformal geometry and its applications on 3d shape matching, recognition, and stitching,* PAMI, 29:7, pp. 1209–1220.
[11] W. Zeng, Y. Zeng, Y. Wang, X. Gu, and D. Samaras, *Non-rigid surface matching and registration based on holomorphic differentials,* 2008.
[12] M. Jin, W. Zeng, F. Luo, and X. Gu, *Computing tëichmuller shape space,* IEEE TVCG, 2008.
[13] P. Shilane, P. Min, M. Kazhdan, and T. Funkhouser, *The princeton shape benchmark,* 2004, pp. 167–178.
[14] N. Iyer, S. Jayanti, K. Lou, Y. Kalyanaraman, and K. Ramani, *Three dimensional shape searching: state-of-the-art review and future trends,* Computer-Aided Design, 37:5 (2005), pp. 509–530.
[15] J. W. Tangelder and R. C. Veltkamp, *A survey of content based 3d shape retrieval methods,* Multimedia Tools and Applications, 2008.
[16] S. Biasotti, L. D. Floriani, B. Falcidieno, P. Frosini, D. Giorgi, C. Landi, L. Papaleo, and M. Spagnuolo, *Describing shapes by geometrical-topological properties of real functions,* ACM Computing Surveys, 40:4 (2008).
[17] X. Gu and S.-T. Yau, *Surface classification using conformal structures,* (2003), pp. 701–708.
[18] M. Jin, F. Luo, S. Yau, and X. Gu, *Surface classification using conformal structures,* (2007), pp. 387–393.
[19] S. Wang, Y. Wang, M. Jin, X. GU, and D. Samaras, *3d surface matching and recognition using conformal geometry,* 2 (2006), pp. 2453–2460.
[20] X. Gu, S. Wang, J. Kim, Y. Zeng, Y. Wang, H. Qin, and D. Samaras, *Ricci flow for 3d shape analysis,* (2007), pp. 1–8.
[21] R.-M. Rustamov, *Laplace-beltrami eigenfunctions for deformation invariant shape representation,* 2007.
[22] P. Xiang, C.-O. Hua, F.-X. Gang, and Z.-B. Chuan, *Pose insensitive 3d retrieval by poisson shape histogram,* 4488 (2007), pp. 25–32.
[23] M. Ben-Chen and C. Gotsman, *Characterizing shape using conformal factors,* Crete, April 2008.
[24] M. S. Floater and K. Hormann, *Surface parameterization: a tutorial and survey,* Springer, pp. 157–186.
[25] A. Sheffer, E. Praun, and K. Rose, *Mesh parameterization methods and their applications,* 2:2 (2006).
[26] X. Gu and S.-T. Yau, *Global surface conformal parameterization,* 43, pp. 127–137.
[27] Y. Tong, S. Lombeyda, A. N. Hirani, and M. Desbrun, *Discrete multiscale vector field decomposition,* 22:3, pp. 445–452.
[28] S. Gortler, C. Gotsman, and D. Thurston, *Discrete one-forms on meshes and applications to 3d mesh parameterization,* 33:2, pp. 83–112.
[29] Y. Tong, P. Alliez, D. Cohen-Steiner, and M. Ddesbrun, *Designing quadrangulations with discrete harmonic forms,* pp. 201–210.
[30] F. Kalberer, M. Nieser, and K. Plothier, *Quadcover-surface parameterization using branched coverings,* 2007.
[31] M. Fisher, P. Schroder, M. Desbrun, and H. Hoppe., *Design of tangent vector fields,* 26:3 (2007), pp. 56–66.
[32] R. S. Hamilton, *Three manifolds with positive ricci curvature,* Journal of Differential Geometry, 17 (1982), pp. 255–306.
[33] B. Chow and F. Luo, *Combinatorial ricci flows on surfaces,* Journal Differential Geometry, 63:1 (2003), pp. 97–129.
[34] F. Luo, *Combinatorial yamabe flow on surfaces,* Commun. Contemp. Math., 6:5 (2004), pp. 765–780.
[35] F. Luo, X. Gu, and J. Dai, *Variational Principles for Discrete Surfaces*,International Press of Boston, August 2008, vol. 4.
[36] M. Jin, J. Kim, F. Luo, and X. Gu, *Discrete surface ricci flow,* IEEE TVCG, 2008.
[37] Y.-L. Yang, J. Kim, F. Luo, and X. Gu, *Optimal surface parameterization using inverse curvature map,* 2008.
[38] S. Boris, P. Schröder, and U. Pinkall, *Conformal equivalence of triangle meshes,* ACM Trans. Graph., 27:3 (2008), pp. 1–11.

[39] M. Ben-Chen, C. Gotsman, and G. Bunin, *Conformal flattening by curvature prescription and metric scaling,* 27:2 (2008).
[40] A. I. Bobenko and B. A. Springborn, *Variational principles for circle patterns and koebe's theorem,* 356 (2004), pp. 659–689.
[41] W. Zeng, X. Yin, Y. Zeng, Y. Wang, X. Gu, and D. Samaras, *3d face matching and registration based on hyperbolic ricci flow,* 2008.
[42] H. M. Farkas and I. Kra, *Riemann Surfaces (Graduate Texts in Mathematics)*, Springer, 1991.
[43] A. Papadopoulos, *Handbook of Tëichmuller Theory*, European Mathematical Society, 2007.
[44] R. Schoen and S.-T. Yau, *Lectures on Differential Geometry*, International Press of Boston, 1994.
[45] T. Chan, P. Thompson, S.-T. Yau, X. Gu, and Y. Wang, *Genus zero surface conformal mapping and its application to brain surface mapping,* TMI, 23:7 (2004).
[46] Y. Wang, M. Gupta, S. Zhang, S. Wang, X. Gu, D. Samaras, and P. Huang, *High resolution tracking of non-rigid 3d motion of densely sampled data using harmonic maps,* (2005), pp. 388–395.